Comparative study of the ELMs between the ECEI observations and BOUT++ simulations in KSTAR H-mode plasma

M. Kim[1], M. J. Choi[1], J. Lee[1], J. E. Lee[1], G. S. Yun[1], W. Lee[2], H. K. Park[2], X. Xu[3], A. Y. Pankin[4], C. W. Domier[5], N. C. Luhmann, Jr.[5] and KSTAR team

[1]*POSTECH, Pohang, Republic of Korea*

[2]*Ulsan National Institute of Science and Technology, Ulsan, Republic of Korea*

[3]*Lawrence Livermore National Laboratory, Livermore, California, USA*

[4]*Tech-X Corporation, Boulder, USA*

[5]*University of California, Davis, California, USA*

Introduction

2D electron cyclotron emission imaging (ECEI) system is advanced diagnostic tool with high temporal and spatial resolution. In KSTAR tokamak, it have observed MHD structure from plasma core to edge; sawtooth [1], tearing mode [2] and ELMs [3]. In case of plasma edge observation, the interpretation of electron cyclotron (EC) emission signal is complicated due to rapidly changing optical thickness and subsequent downshifted emission spectra. To provide confidence on observations, the observed structure is compared with synthetic images which are constructed from results of numerical simulation code, BOUT++ [4]. Based on the reliability of edge observation, the peeling-ballooning stability model can be examined using experimental observations and edge stability simulation codes.

ELM observations and BOUT++ simulation

The KSTAR discharge #7328 is typical ELMy H-mode discharge heated by neutral beam of power ~ 3 MW. The basic parameters are I_p = 750 kA, B_T = 2.25 T and q_{95} ~ 5 at the current flat top. Fig. 1(a) shows the ELM structure observation of ECEI system during inter-ELM period. The observed structure sustains the coherent structure until the crash time. In KSTAR, the toroidal mode number n of the ELM structure can be determined by toroidal

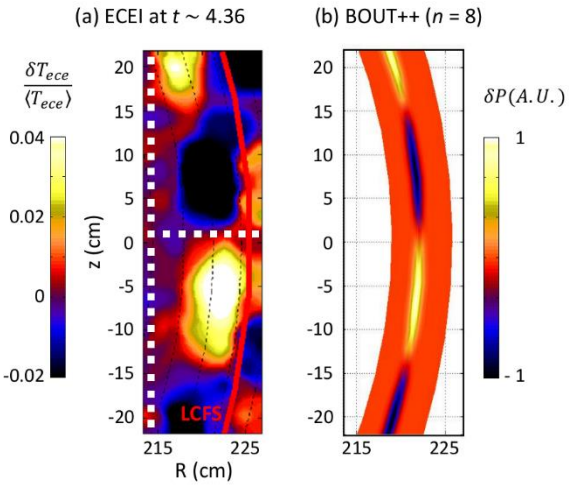

Figure 1 (a) ECEI observation in KSTAR discharge #7328 at t ~ 4.36 s. Square: 24 X 8 channel positions of ECEI system (b) n = 8 mode structure from BOUT++ simulation

Mirnov coil array or two toroidally-separated ECEI system [5]. In here, the toroidal mode number of observed structure is $n = 8$.

Because the profile information at the pedestal region is not enough to reconstruct pedestal structure, the pedestal pressure profile is assumed such that $n = 8$ mode is most unstable in BOUT++ linear stability analysis [6]. In here, three-field model (pressure, magnetic potential and vorticity) was employed [4]. The pressure at the pedestal top is estimated by measure T_e by ECE radiometry and estimated n_e from line averaged density. The obtained $n = 8$ ELM structure from BOUT++ simulation is illustrated in Fig. 1(b). Radial mode widths in two cases differ considerably. To explain this difference, a synthetic process is introduced.

Synthetic image reconstruction

The images from BOUT++ simulation are converted to the synthetic 2D images through synthetic diagnostic system. Synthetic diagnostic considers characteristics of EC emission at certain plasma position and instrumental effects when the emission is detected by each ECEI channels. The synthetic temperature T_{syn} of a particular synthetic diagnostic channel is determined by the simulated temperature T_e(R, z) with vertical and radial response function f(R), g(z), respectively;

$$T_{\mathrm{syn}} = \frac{\int_{\Delta R}\int_{\Delta z} T_e(R,z) f(R) g(z)\, \mathrm{dR dz}}{\int_{\Delta R}\int_{\Delta z} f(R) g(z)\, \mathrm{dR dz}} \qquad (1)$$

In Eq. (1), temperature T_e(R, z) is deduced from the pressure P in simulation, the vertical response function g(z) is vertical response pattern of ECEI antenna. The radial response function f(R) is determined by EC emission theory including relativistic downshift effects [7-9]. Fig. 2(a) illustrates bandwidth of each radial channel assumed to be simple rectangular shape (dotted line) and radial response function of corresponding channel including relativistic effects (solid line). The radial response function gets broader due to the relativistic broadening. In case of channels outside the separatrix (R > 224), the emission from cold resonance position is dominated by

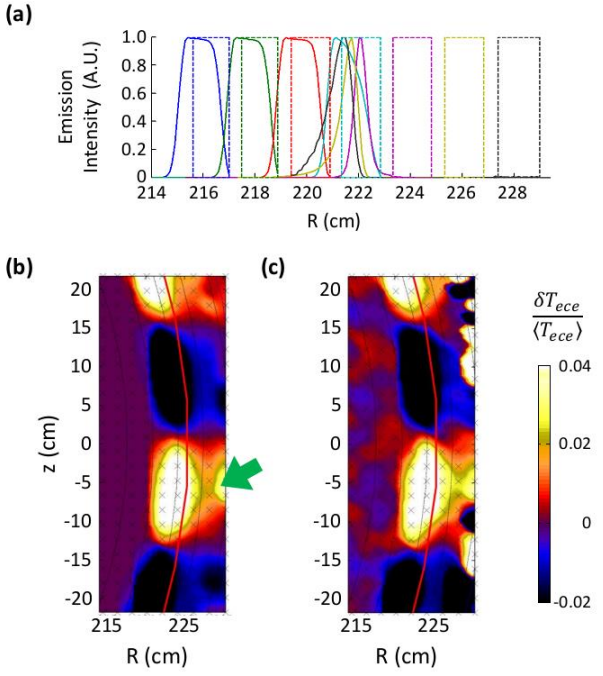

Figure 2 (a) Dotted line: bandwidth of each radial channel; solid line: response function of each radial function including relativistic effect at outer mid-plane (b) Synthetic image from BOUT++ simulation result. Phantom image (arrow) of the ELM appears outside the separatrix (c) Synthetic image including system noise

the downshifted signals. Fig. 2(b) shows the reconstructed synthetic image. The radial mode size is comparable to that in observed one and clear phantom image (indicated by arrow) outside the separatrix appears. To make a more realistic image, the system background noise is considered (Fig. 3(c)). Because the signal level of the phantom image is comparable to the noise level, it is difficult to distinguish the phantom image from the noise. This successful reconstruction indicates that the observed structure at the plasma edge is ELM structure expected by the peeling-ballooning model.

Comparison with peeling-ballooning model

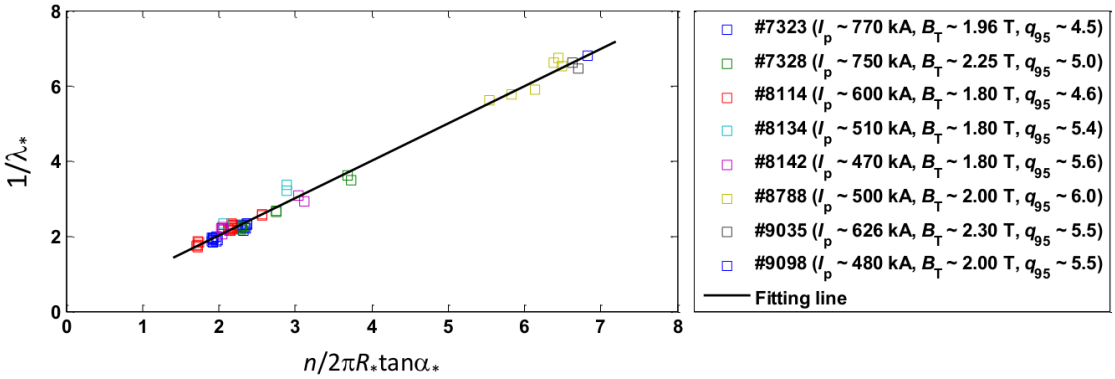

Figure 3 The observed poloidal mode spacing at outer mid-plane λ_* is related by $1/\lambda_* = n(2\pi R_* \tan\alpha_*)^{-1}$ where n is toroidal mode number, R_* is major radius and α_* is pitch angle at outer mid-plane. The wide range of toroidal mode number has been observed in various discharge.

During the investigation of ELM dynamics for the comparative study, the wide range of toroidal mode number ($4 < n < 14$) was observed in various H-mode discharge. The poloidal mode spacing at outer mid-plane λ_* can be measured by the ECEI observation results. The measured λ_* is related with toroidal mode number n by $1/\lambda_* = n(2\pi R_* \tan\alpha_*)^{-1}$ where asterisk represents the quantities at outer mid-plane, R is major radius and α is pitch angle of magnetic field [5]. The set of observation was well matched with this relation (Fig. 3). Based on the observation in wide range of n, peeling-ballooning model can be investigated wherever plasma pedestal condition is peeling or ballooning dominant. Fig. 4 illustrates the results of peeling-ballooning stability analysis when ELM structure in Fig. 1 is observed. Because pressure profile at the plasma edge is not fully measured at the moment, the pedestal condition could not be mapped into J-α space in peeling-ballooning diagram. However, we can guess the pedestal condition using the observation of $n = 8$ ELM structure. In the coming KSTAR operation, the plasma operating position on J-α space can be estimated using measure pressure profile and estimated current density including bootstrap current. The peeling-ballooning model can be investigated using the ECEI ELM observations.

Summary

The ELM observation by ECEI system should be carefully investigated because the interpretation of EC emission at the edge of plasmas is complex due to rapid change of optical thickness. The synthetic image obtained from the result of BOUT++ ELM simulation is compared with the observed images. The synthetic process reconstructs observed image by considering radial and vertical instrumental broadening and relativistic down-shift of EC emission. Based on the confidence of observation, the peeling-ballooning model will be investigated with improved pedestal profile measurements in coming KSTAR campaign.

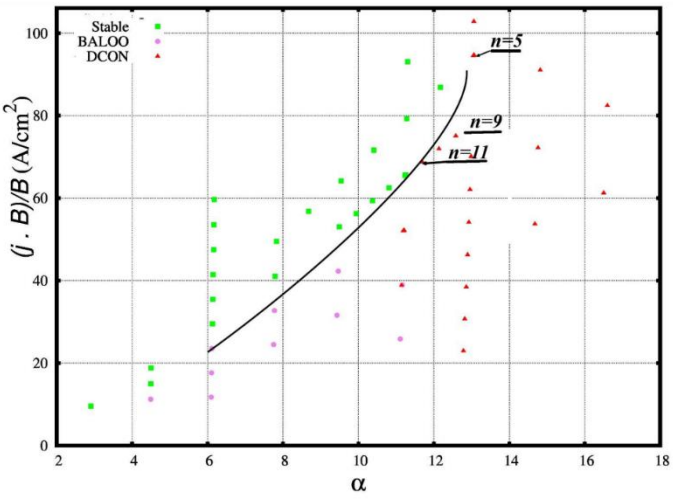

Figure 4 Peeling-ballooning stability analysis results at #7328 $t \sim 4.36$ s. The peeling-ballooning model can be investigated using ECEI ELM observations with pedestal profiles.

Acknowledgement

This research was supported by NRF of Korea under contract no. 2009-0082507 and US DOE under contracts DE-AC52-07NA27344 at LLNL, DE-FG02-99ER54531 at UC Davis, and DE-SC0006629 at Tech-X.

Reference

[1] H. K. Park et al., Phys. Rev. Lett., 96, 195003 (2006)

[2] Minjun J. Choi, et al., Nucl. Fusion, 54, 083010 (2014)

[3 G. S. Yun et al., Phys. Rev. Lett., 107, 045004 (2011)

[4] B. D. Dudson et al., Computer Physics Comm., 180, 1467 (2009)

[5] J. Lee, et al., it will be published in Review of Scientific Instruments (2014)

[6] X. Q. Xu et al., Nucl. Fusion, 51, 103040 (2011)

[7] I. H. Hutchinson, 'Principles of Plasma Diagnostics', Cambridge University Press (1987)

[8] G. Bekefit, 'Radiation Processes in Plasmas', Wiley, New York (1966)

[9] M. Kim, et al., it was submitted to Nuclear Fusion (2014)